Journal of AppliedMath 2024, 2(6), 1593.
https://doi.org/10.59400/jam1593

Article

Site effects in seismic motion

Bogdan Felix Apostol

Institute of Earth's Physics, 077125 Magurele, Romania; afelix@theory.nipne.ro

CITATION

Apostol BF. Site effects in seismic motion. Journal of AppliedMath. 2024; 2(6): 1593. https://doi.org/10.59400/jam1593

ARTICLE INFO

Received: 15 August 2024
Accepted: 13 September 2024
Available online: 26 December 2024

Abstract: We use the harmonic-oscillator model to analyze the motion of the sites (ground motion), seimograph recordings, and structures built on the Earth's surface under the action of the seismic motion. The seismic motion consists of singular waves (spherical-shell P and S primary seismic waves) and discontinuous (step-wise) seismic main shocks. It is shown that these singularities and discontinuities are present in the ground motion, seismographs' recordings and the motion of the built structures. In addition, the motion of the oscillator exhibits oscillations with its own eigenfrequency, which represent the response of the oscillator to external perturbations. We estimate the peak values of the displacement, the velocity and the acceleration of the ground motion, both for the seismic waves and the main shock, which may be used as input parameters for seismic hazard studies. We discuss the parameters entering these formulae, like the dimension of the earthquake focus, the width of the primary waves and the eigenfrequencies of the site. The width of the seismic waves on the Earth's surface, which includes the energy loss, can be identified from the Fourier spectrum of the seismic waves. Similarly, the eigenfrequencies of the site can be identified from the spectrum of the site response. The paper provides a methodology for estimating the input parameters used in hazard studies.

Keywords: seismic motion; site response; seismograph recordings; spectral response; seismic hazard

1. Introduction

The estimation of the local ground motion produced by earthquakes is the central theme of the seismic hazard studies. The current procedure employs empirical ground-motion equations, which provide the quantities of interest, like peak ground acceleration (velocity, displacement), for a given earthquake magnitude and focal and epicentral distances [1]. The parameters of these equations are fixed by simulating the effects of reference earthquakes. For local motion the problem is complicated by the inhomogeneities of the Earth's surface. Random vibration theory and stochastic simulations are used, which have the advantage of including more realistic features and assessing the estimation errors [2–5]. Knowledge gained by such methods is incorporated in building codes [6], source parameters and scaling relations are used for estimation the seismic hazard [7] and numerical modelling is extensively used to this end [8]. The stochastic methods have recently been improved [9] and fractal dimension modelling was employed [10]. The current studies of seismic hazard are based on the so-called ground motion predicting equations, which are empirical equations, obtained by fitting data and extrapolating them to cases of interest. There exist at this moment hundreds of such equations, which should be selected for particular

problems, the relevant parameters identified, their accuracy assessed, and updated almost continuously. In spite of these difficulties, the ground motion predicting equations remain a valuable tool. Although important advances have been made in this direction [11–13], a need for improvement of the techniques is often felt [14]. We give in the present paper another method of estimating the peak values of the ground motion, which could be useful in seismic hazard studies. It is based on a theoretical model previously published. Although the number of cases on which we have tested this method is rather limited, the results are promising.

Recently, we introduced the tensorial force which acts in a localized seismic focus [15, 16]. This force is a product of the tensor of the seismic moment, a temporal δ-function and the spatial derivatives of a δ-function. Assuming that the Earth is a homogeneous and isotropic elastic medium, we derived the P and S primary seismic waves. These waves are spherical shells, with a scissor-like shape, which propagate with the velocities of the elastic waves. Once arrived at the Earth's surface, the primary waves generate secondary wave sources on the surface, according to Huygens' principle, which produce secondary waves. On the Earth's surface the secondary waves have the shape of two superposed abrupt walls, with a long tail, propagating with the velocities of the elastic waves, behind the propagating spot of the primary waves on the Earth's surface. These two walls form the seismic main shock. All these results are in qualitative agreement with the recorded seismograms (a problem known sometimes as the seismological, or Lamb, problem). Apart from these general features, the recordings exhibit oscillations, such that the results described above look like overall (envelope) characteristics of the recorded seismic motion.

The assumption of a homogeneous and isotropic elastic medium implies a spatial average of the elastic properties. As long as we limit ourselves to overall features, this is a satisfactory assumption. If we are interested in the local motion, we need to take into account the elastic particularities of the site. This problem occurs for the local inhomogeneities on the Earth's surface, or the inertial motion of a seismograph, or the motion of a structure built on the Earth's surface. We can view a site as a portion of an elastic medium, connected to its surroundings by elastic forces. It may have an oscillatory motion of its center of mass, it may exhibit coupled oscillations of its internal structural elements, or it may display vibrations with multiple eigenfrequencies, depending on the boundary conditions. Under the action of the seismic motion, like the P and S seismic waves, or the main shock, the site exhibits its own seismic response. The original seismic motion is superposed over the site response, the resulting motion being the ground motion. We may neglect in the first approximation the coupling of the internal degrees of freedom, and view the site as a (damped) linear harmonic oscillator (with one degree of freedom). A refined model may include a superposition of linear harmonic oscillators. A similar problem, also presented in this paper, can be formulated for a seismograph, or a built structure, where the original motion (perturbation) is the ground motion.

We examine in this paper the motion of a harmonic oscillator under the action of the seismic motion, or the ground motion. The resulting motion is the ground motion, or the seismograph recordings, or the motion of a built structure, respectively. The

results depend on the eigenfrequency of the oscillator, such that the spectral components of the motion, which imply Fourier transforms, can give valuable information about the characteristics of the site. If we are able to determine the resulting motion, like the ground motion, from the parameters of the earthquake, we could have a procedure which could be useful for the seismic hazard studies. This is what we attempt in the present paper.

Before entering details, an introductory summary may be helpful.

The paper presents results which may be relevant for both the theoretical insight into the site effects of the seismic motion and useful for seismic hazard studies. Mainly, it responds to the following question: Suppose that we expect an earthquake, with a certain magnitude, at a certain place. How big will the displacement, velocity, acceleration be at that place? The answer is usually provided by the so-called peak values. Such a knowledge is useful as input parameters for studies of seismic hazard. In order to answer this question, as accurately and reliable as possible, we need 1) to know how, quantitatively, the seismic motion is, 2) what the local site effects are, and, additionally, what kind of effects such a motion will have on a built structure on the Earth's surface.

The answer to question 1) is provided by our previously published papers, cited herein wherever necessary. The results of these works are cast in the present paper in a form suitable for numerical estimation. As it is well known, a seismic motion consists of two P and S primary waves and a main shock. We work out suitable formulae for the peak values for all these three types of motion. We find out that, apart from the elastic constants of the place (e.g., elastic waves velocity), the peak values depend on the distance R to the earthquake focus, the epicentral distance r, a parameter l of the order of the dimension of the focal region and another parameter length l_0, which includes the effects of dissipation. We assume that we know R and r. Also, we show that the length l is given by the magnitude of the earthquake, as established in our previosly published papers. It remains to know l_0.

At this moment the problem is complicated by the specific nature of the local site, i.e. question 2) above. We give arguments in this paper that we may know, model, the behaviour of the site. We present detailed calculations for the simplest case where the site can be modelled as a harmonic oscillator with its own eigenfrequency ω_g. More sophisticated calculations can be done, but the main, qualitative effect is already included in such a simplified model. The peak values should be modified according to this site reponse, and we present in the paper the corresponding calculations. Now, the peak values depend on ω_g and l_0, and we need know these parameters. We have access to the ground motion through seismographs measurements. Therefore, we need know the seismographs response, so we calculate this motion, and present the results in this paper. We show in this paper that the Fourier transform of the seismograph response provides the parameters ω_g and l_0. Finally, we have now the desired peak values. We include calculations of the response of a built structure, because, on one hand, these calculations are similar with those already described, and, on the other, it is not very often that they are correctly, and rigorously known; we include them herein for reference and completeness.

This is, basically, the contents and the philosophy of this paper. We do not claim that our results are exhaustive. They may be extended and improved in many directions. But we claim that we present a new methodology for estimating the seismic hazad on a rigorous basis.

A shorter summary is as follows: the effects of the seismic motion, as recorded by seismographs, include the site response. Typical seismic motion consists of P and S seismic waves and the seismic main shock. Besides the specific patterns of these movements, the seismographs record many oscillations. We show that these oscillations arise from site and seismographs' eigenfrequencies. The sites and the seismographs are modelled as damped linear harmonic oscillators. We present an analysis for a single oscillating mode. This analysis allows us to estimate the peak values of the local displacement, velocity and acceleration, as functions of the characteristics of the earthquake. The spectrum of the seismograph recordings provides additional information about the intervening parameters. Such values can be used as input parameters in studies of seismic hazard. The paper presents the quantitative analysis of the site response in terms of the earthquake characteristics, and, on the other hand, as an application, it provides a methodology for estimating the input parameters in hazard studies.

2. P and S seismic waves

We consider an earthquake focus localized at the origin; we assume that the seismic activity in the focus during an earthquake lasts a short time T. The density of the tensorial force acting in the focus is $f_i = (M_{ij}/\rho)T\delta(t)\partial_j\delta(\boldsymbol{R})$, where M_{ij} are the cartesian components of the seismic-moment tensor and ρ is the density of the elastic medium [15, 16]. According to these References, the P and S seismic-wave displacement in a homogeneous and isotropic elastic medium is given by

$$\begin{aligned} \boldsymbol{u}_P &= -\tfrac{TM_4}{4\pi\rho c_l^3 R}\boldsymbol{n}\delta'(t-R/c_l)\ , \\ \boldsymbol{u}_S &= -\tfrac{T(M_4\boldsymbol{n}-\boldsymbol{M})}{4\pi\rho c_t^3 R}\delta'(t-R/c_t) \end{aligned} \tag{1}$$

where $M_i = M_{ij}n_j$, $M_4 = M_in_i = M_{ij}n_in_j$, $c_{l,t}$ are the (longitudinal and transverse) velocities of the elastic waves and $\boldsymbol{n} = \boldsymbol{R}/R$ is the unit vector from the focus to the observation point. The observation point is placed at position $\boldsymbol{R}$ from the focus and the displacement is computed at time t. We can see that these displacements are spherical-shell waves, with a scissor-like shape, propagating with velocities $c_{l,t}$. The P wave is longitudinal, while the S wave is transverse. We call them primary seismic waves.

The functions $\delta(t-R/c_{l,t})$ are viewed as having the value $1/T$, localized over a range $\Delta t = T$ from $-T/2$ to $T/2$ at the central moment of time $t = R/c_{l,t}$. For local motion we prefer to consider this moment of time as the origin, and use the lengths $l_{l,t} = c_{l,t}T$. Then, the functions $\delta(t-R/c_{l,t})$ have the peak value $c_{l,t}/l_{l,t}$ and extend from $-l_{l,t}/2c_{l,t}$ to $l_{l,t}/2c_{l,t}$. Similarly, we might say that the functions $\delta'(t-R/c_{l,t})$ entering Equation (1) have the values $\pm 2c_{l,t}^2/l_{l,t}^2$, peaked over the ranges $-l_{l,t}/2c_{l,t}$ to

0 and 0 to $l_{l,t}/2c_{l,t}$; the functions $\delta'(t - R/c_{l,t})$ have a scissor-like shape.

The lengths $l_{l,t}$ may be viewed as a measure of the dimension of the focus, according to the expression of the tensorial force given above. It is shown that we can get the seismic-moment tensor, the energy (and the magnitude) of an earthquake and the focal volume from measurements of the amplitudes of the displacements $\boldsymbol{u}_{P,S}$ made on the Earth's surface (a problem known as the inverse seismological problem) [17]. From the focal volume we can have an estimate of the dimension l of the focus, which is of the same order of magnitude as $l_{l,t}$. According to these References, inside the localized focal volume of dimension l, the focus has the structure of a shearing fault, as provided by the Kostrov representation [17].

For practical purposes we can use in Equation (1) average values of the physical quantities. For instance, we can use an average velocity c for $c_{l,t}$; if $c_l = 3$ km/s and $c_t = 7$ km/s, we may use $c = 5$ km/s (which would imply an error of 40%). Also, the Earth's density can be taken $\rho = 5$ g/cm^3. Moreover, we can limit ourselves to the magnitudes $u_{P,S}$ of the displacements, and use an average value of the seismic-moment tensor $\overline{M} = (M_{ij}^2)^{1/2}$ for M_4 and $M_4\boldsymbol{n} - \boldsymbol{M}$. This magnitude of the seismic-moment tensor is related to the energy E of the earthquake through $\overline{M} = 2\sqrt{2}E$ [16,17]. On the other hand, we can relate the magnitude of the seismic-moment tensor (in erg) to the moment magnitude M_w of the earthquake, through the Hanks-Kanamori relation

$$\lg \overline{M} = \frac{3}{2}M_w + 16.1 \tag{2}$$

Under these conditions, $l_{l,t} = l$ and we can use

$$u = u_0 l\delta'(t - R/c) \ , \ u_0 = \frac{\overline{M}}{4\pi\rho c^4 R} \tag{3}$$

for the magnitude of the displacement of a generic primary seismic wave. We can see that if we know the earthquake magnitude and the focal distance, together with the elastic constants of the medium and the length l, we can estimate the peak displacement (u_{max}), velocity (v_{max}) and acceleration (a_{max}), by taking the time derivatives of the function $\delta(t)$ for $t \simeq R/c$.

The time derivatives of the δ-function can be computed according to the discussion given above, where the function $\delta(t)$ has a peak value c/l and extends from $-l/2c$ to $l/2c$, the function $\delta'(t)$ has the peak values $\pm 2c^2/l^2$ in the intervals $-l/2c$ to 0 and 0 to $l/2c$, and so on. For instance, the maximum values of the δ-function and its derivatives are $\delta_{max} = c/l$, $\delta'_{max} = 2c^2/l^2$, $\delta''_{max} = 8c^3/l^3$ and $\delta'''_{max} = 64c^4/l^4$. However, this fine structure of the derivatives of the δ-function is uncertain, in view of the definition of the δ-function as a function localized over a very short distance l. We prefer to use the estimations $\delta_{max} = c/l$, $\delta'_{max} = c^2/l^2$, $\delta''_{max} = c^3/l^3$ and $\delta'''_{max} = c^4/l^4$.

It is shown that the average seismic-moment tensor (which is proportional to the released energy) can be represented as $\overline{M} = 4\sqrt{2}\rho c^2 l^3$ [18], such that $u_0 = \sqrt{2}l^3/\pi c^2 R$ and

$$u = \frac{\sqrt{2}l^3}{\pi c^2 R}\left[l\delta'(t)\right] \tag{4}$$

where we choose the origin of the time at R/c. In Equation (4) we may replace $l\delta'(t)$ by c^2/l, such that we get the approximate formulae

$$u_{max} = \frac{\sqrt{2}l^2}{\pi R} \ , \qquad v_{max} = \frac{\sqrt{2}cl}{\pi R} \ , \ a_{max} = \frac{\sqrt{2}c^2}{\pi R} \tag{5}$$

For a given magnitude in Equation (2) and by making use of $\overline{M} = 4\sqrt{2}\rho c^2 l^3$ we can get the parameter l, such that we have an estimate of the peak values of the seismic motion produced by the primary waves from the above equations. By making use of $\rho = 5$ g/cm^3 and $c = 5$ km/s in Equation (2), we get

$$\lg l = \frac{1}{2}M_w + 1 \tag{6}$$

(in cm). For instance, for an earthquake with magnitude $M_w = 7$ we get $\overline{M} = 4 \times 10^{26}$ erg, $l = 316$ m, $u_0 = 57/R$ (cm) and u_{max} (cm)$= 4.5 \times 10^8/R$ (cm), v_{max} (cm/s)$= 7 \times 10^9/R$ (cm), a_{max} (cm/s^2)$= 10^{11}/R$ (cm) for the numerical data given above ($\rho = 5$ g/cm^3, $c = 5$ km/s). Equation (6) is a basic equation for our purpose.

The above formulae include the energy loss of the waves propagating through the medium, except for the shape of the δ-fuction, which is modified as [19]

$$\delta(t) \to \frac{1}{\pi}\frac{\alpha}{t^2 + \alpha^2} \tag{7}$$

where α is an energy-loss parameter. The spatial extension of this function is approximately $l_0 = 2\alpha c/\sqrt{3} > l$. We may assume that the product $l_0\delta(t)$, where $\delta(t)$ is given by Equation (7), remains c, such that $l_0\delta'(t)$ should be replaced by c^2/l_0. The length l_0 is related to the width of the function given by Equation (7). We call this parameter the width of the primary seismic waves. We view l_0 as an average parameter for the primary waves. By introducing the parameter l_0, the peak values given by Equation (5) are diminished, according to the equations

$$u_{max} = \frac{\sqrt{2}l^3}{\pi l_0 R} \ , \qquad v_{max} = \frac{\sqrt{2}cl^3}{\pi l_0^2 R} \ , \ a_{max} = \frac{\sqrt{2}c^2 l^3}{\pi l_0^3 R} \tag{8}$$

We note that the elastic energy of the seismic waves is proportional to l^3 ($\sim \dot{u}^2 \times l$, Equation (5)), such that it is reduced in Equation (8) by the energy-loss factor $(l/l_0)^3$. This is precisely the factor entering the acceleration in Equation (8). The earthquake parameters determined from the inverse seismological problem (where the displacement is employed) are not affected by the parameter l_0, but the effect of this parameter on the peak values, especially the maximum acceleration, is important. We shall see in the next sections how this parameter can be determined from the Fourier spectrum of the seismograms. According to its definition, we expect the ratio l/l_0 to depend sightly on position and magnitude, though non-linear effects for higher magnitudes may give a more appreciable dependence.

3. Ground motion produced by primary waves

Let us consider a linear harmonic oscillator with coordinate u_{osc}, frequency ω_g and damping coefficient γ_g. Its equation of motion is

$$\frac{d^2}{dt^2}u_{osc} + \omega_g^2(u_{osc} - u^0) + 2\gamma_g \frac{d}{dt}(u_{osc} - u^0) = 0 \tag{9}$$

where u^0 is the fixed equilibrium coordinate. In the presence of the seismic motion the equilibrium coordinate acquires a displacement u, as given, for instance, by Equation (3) for primary waves, such that Equation (9) becomes

$$\frac{d^2}{dt^2}u_{osc} + \omega_g^2(u_{osc} - u^0 - u) + 2\gamma_g \frac{d}{dt}(u_{osc} - u^0 - u) = 0 \tag{10}$$

We are interested in the relative coordinate $u_r = u_{osc} - u^0 - u$, for which Equation (10) can be written as

$$\ddot{u}_r + \omega_g^2 u_r + 2\gamma_g \dot{u}_r = -\ddot{u} \tag{11}$$

We can see that an inertial force $-\ddot{u}$ occurs (per unit mass), as expected.

In general, the equation

$$\ddot{u}_r + \omega_g^2 u_r + 2\gamma_g \dot{u}_r = S(t) \tag{12}$$

where $S(t)$ is a source term, defined for $t > 0$, can be solved by using the Green function G which satisfies the equation

$$\ddot{G} + \omega_g^2 G + 2\gamma_g \dot{G} = \delta(t) \tag{13}$$

a particular solution is given by

$$u_r(t) = \int_0^\infty dt' G(t - t') S(t') \tag{14}$$

We look for causal solutions, which are vanishing for $t < 0$. The Green function is obtained from Equation (13), by using a Fourier transformation, and placing the poles in the lower ω-plane of integration ($\gamma_g > 0$). For $\gamma_g \ll \omega_g$ we get

$$G(t) = \theta(t) \frac{\sin \omega_g t}{\omega_g} e^{-\gamma_g t} \tag{15}$$

and

$$u_r(t) = \frac{1}{\omega_g} \int_0^t dt' e^{-\gamma_g (t - t')} \sin \omega_g (t - t') S(t') \tag{16}$$

(for $t > 0$); we can verify the vanishing initial conditions.

However, the most direct method of solving the equation

$$\ddot{u}_r + \omega_g^2 u_r + 2\gamma_g \dot{u}_r = -u_0 l \delta'''(t) \tag{17}$$

for the source term given by the primary waves (Equation (10)) is to compare it to

Equation (13) for the Green function. We get immediately

$$u_r(t) = -u_0 l G'''(t) = u_0 l \omega_g^2 e^{-\gamma_g t} \cos \omega_g t \tag{18}$$

for $t > 0$ and $\gamma_g \ll \omega_g$. This is the response of the oscillator to the initial perturbation produced by the primary waves. In addition, by integrating Equation (17) over a small interval around $t = 0$, we get

$$u_r(t) = -u_0 l \delta'(t) \tag{19}$$

which is the initial displacement with the minus sign $-u(t)$, as expected from $u_r = u_{osc} - u^0 - u$. Putting together these two contributions, we get the ground-motion displacement

$$u_g(t) = u_0 l \left[-\delta'(t) + \theta(t) \omega_g^2 e^{-\gamma_g t} \cos \omega_g t\right] \tag{20}$$

under the action of the primary waves. It is worth noting that for $\omega_g = 0$, i.e. for a site identical with the medium, the displacement is the (singular) seismic motion with the minus sign, as expected.

We can see that the site motion is a damped oscillation with frequency ω_g (the response), superposed over the perturbing scissor-like seismic motion. The shape of the function $u_g(t)$ depends on the ratio of the two characteristic frequencies c/l and ω_g. If $c/l \gg \omega_g$, we have an abrupt scissor-like (seismic) motion, followed by damped oscillations with frequency ω_g; if $c/l \ll \omega_g$, we have damped oscillations with a slowly-varying envelope. A schematic representation of the ground-motion displacement (Equation (20)) is shown in **Figure 1**. From Equation (20) we can estimate a maximum displacement of the ground

$$u_{gmax}^p = u_{max} \left(1 + l^2 \omega_g^2 / c^2\right) \tag{21}$$

where the upper label p stands for "primary". Similarly, we can estimate the peak values of the ground-motion velocity and acceleration produced by the primary waves

$$v_{gmax}^p = v_{max} \left(1 + l^3 \omega_g^3 / c^3\right) \ , \ a_{gmax}^p = a_{max} \left(1 + l^4 \omega_g^4 / c^4\right) \tag{22}$$

where u_{max}, $v_{max}$and a_{max} are given by Equation (8).

We may assume that the eigenfrequencies of a site with dimension L are of the order $\omega_g = cn/L$, where $n = 1, 2, 3...$, such that $l\omega_g/c \simeq ln/L$; usually, only the lowest frequencies are excited, such that, since $l/L \ll 1$, we may view the $l\omega_g/c$-terms in the above equations as small corrections. If we take into account the energy loss, the length l should be replaced by l_0 in the above equations. We can see that the site should be defined such that its dimension L is much larger than l_0 ($L \gg l_0$). By making use of Equation (8) we get

$$u^p_{gmax} = \frac{\sqrt{2}l^3}{\pi l_0 R}\left(1 + l_0^2\omega_g^2/c^2\right) \ ,$$

$$v^p_{gmax} = \frac{\sqrt{2}cl^3}{\pi l_0^2 R}\left(1 + l_0^3\omega_g^3/c^3\right) \ , \tag{23}$$

$$a^p_{gmax} = \frac{\sqrt{2}c^2l^3}{\pi l_0^3 R}\left(1 + l_0^4\omega_g^4/c^4\right)$$

These are the second set of basic equations for our purpose. The ground motion acts as an external force for seismographs' recordings. Both the eigenfrequencies ω_g and the width l_0 of the primary waves can be determined from the spectral analysis of these recordings, as we show in the next sections. Therefore, we need first to compute the motion of the seismograph.

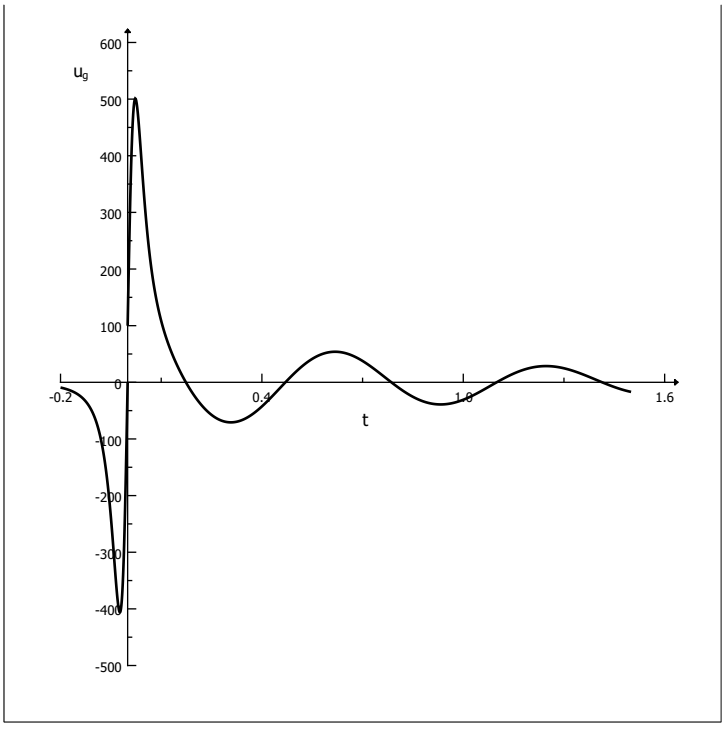

Figure 1. Schematic representation of the ground-motion displacement given by Equation (20) with parameters $\omega_g = 10\ \mathrm{s}^{-1}$, $\gamma_g = 1\ \mathrm{s}^{-1}$ and an extension of the delta function $T = 0.04$ s.

4. Seismograph recordings of the primary waves

We assume that the motion of a seismograph is governed by the equation of a linear oscillator with frequency ω_s and damping coefficient γ_s. The inertial force acting upon the seismograph (per unit mass), i.e. the source term in its equation, is $-\ddot{u}_g$, where u_g is the displacement of the site where the seismograph is placed. By making use of Equation (20), we get

$$-\ddot{u}_g = u_0 l\delta'''(t) - u_0 l\left[\delta'(t) - \omega_g^2\theta(t)\right]\omega_g^2 e^{-\gamma_g t}\cos\omega_g t \tag{24}$$

(for $\gamma_g \ll \omega_g$). By similar calculations as those presented above, we find that the singular terms in Equation (24) ($\sim \delta'''(t),\ \delta'(t)$) give a displacement

$$u_s^{(1)}(t) = u_0 l \left[\delta'(t) - \theta(t)\left(\omega_s^2 + \omega_g^2\right) e^{-\gamma_s t} \cos \omega_s t\right] \tag{25}$$

For the second term in Equation (24) we use Equation (16), which leads to

$$u_s^{(2)}(t) = \theta(t) u_0 l \omega_g^4 A \tag{26}$$

where

$$A = \frac{\omega_g^2 - \omega_s^2}{(\omega_g^2 - \omega_s^2)^2 + 4\omega_g^2(\gamma_g - \gamma_s)^2} \cdot$$

$$\cdot \left(e^{-\gamma_s t} \cos \omega_s t - e^{-\gamma_g t} \cos \omega_g t - \frac{\gamma_g - \gamma_s}{\omega_s} e^{-\gamma_s t} \sin \omega_s t\right) + \tag{27}$$

$$+ \frac{2\omega_g(\gamma_g - \gamma_s)}{(\omega_g^2 - \omega_s^2)^2 + 4\omega_g^2(\gamma_g - \gamma_s)^2} \left(\frac{\omega_g}{\omega_s} e^{-\gamma_s t} \sin \omega_s t - e^{-\gamma_g t} \sin \omega_g t\right)$$

for $\gamma_{g,s} \ll \omega_{g,s}$. We note the presence of the seismic-motion term in seismographs' recordings (the term $\sim \delta'(t)$ in Equation (25)) and the superposed seismograph's response, which consists of damped oscillations with frequencies $\omega_{g,s}$. The term A can also be obtained from the general solution of the equation of the harmonic oscillator with vanishing initial conditions. If we take into account the change in shape of the δ-function, the parameter l in the above formulae should be replaced by l_0.

The solution given above is also valid for a structure with eigenfrequency ω_s, built on a site characterized by frequency ω_g. We note the resonance for $\omega_s = \omega_g$ in Equation (27), as expected.

5. Spectral content of the primary waves

The Fourier transform of the seismograph response given by Equations (25) and (26) includes peaks at frequencies $\omega_{g,s}$. From these Fourier transforms we can read the characteristic frequency of the site ω_g, which is an input parameter for seismic hazard studies. This is another basic information for our purpose. The Fourier transform of the primary waves recorded by seismographs,

$$u_s(t) = u_0 l \delta'(t) \tag{28}$$

(Equation (25)), is of particular interest. If we restore the origin of time R/c, this displacement reads

$$u_s(t) = u_0 l \delta'(t - R/c) \tag{29}$$

The Fourier transform of this function is

$$u_s(\omega) = u_0 l R e \int dt \delta'(t - R/c) e^{i\omega t} = u_0 l \omega \sin \frac{\omega R}{c} \tag{30}$$

We recall that $\delta'(t - R/c)$ has a value of the order c^2/l^2 in the small interval l/c. This amounts to give an indeterminacy of the order $\pm l/2$ to the position R, which produces an indeterminacy $\delta u_s(\omega) \simeq \pi u_0 c \cos \frac{\pi R}{l} \sin(\omega l/2c)$. This is in agreement

with the fact that the frequencies of the seismic waves are smaller than a maximum value of the order c/l (cutoff, corner frequency [20]).

This result can also be obtained by taking the Fourier transform of the function given by Equation (28),

$$u_s(\omega) = u_0 l \int_{-T/2}^{T/2} dt\delta'(t) \sin\omega t =$$

$$= u_0 l \left(-\frac{T}{2}\frac{2}{T^2} \sin\frac{\omega T}{2} - \frac{T}{2}\frac{2}{T^2} \sin\frac{\omega T}{2}\right) = \tag{31}$$

$$= -2cu_0 \sin\frac{\omega l}{2c}$$

(to be compared wih the result given above). It follows that the spectrum of the displacement of the seismic motion exhibits a maximum value for $\omega_m = \pi c/l$ (period $T_m = 2l/c$). The corresponding Fourier transforms of the velocity and acceleration are $v_s(\omega) = \omega u_s(\omega)$ and $a_s(\omega) = \omega^2 u(\omega)$. The velocity spectrum has a maximum at $\simeq 4c/l$ and the acceleration spectrum has a maximum at $\simeq 3\pi c/2l$ (period $\simeq 4l/3c$). By using these maxima values we can obtain an estimation of the dimension l of the focus, which is another input parameter for the seismic hazard studies. Actually, if we take into account the energy loss the length determined from the spectral maximum is l_0. This maximum of the Fourier transform of the seismogram provides another basic information (l_0).

The above result can be applied to the spectrum u_s^P of the P wave, by using $c = c_l$. The S wave has a time delay $\delta = R/c_t - R/c_l$ with respect to the P wave. Consequently, the Fourier transform is given by

$$u_s^S(\omega) = u_0^S l \cos\omega\delta \int_{-T/2}^{T/2} dt\delta'(t) \sin\omega t = -2c_t u_0^S \cos\omega\delta \sin\omega l/2c_t \tag{32}$$

(where $T = l/c_t$). This function has a maximum at $\omega_m^S \simeq \pi c_t/l$, which implies a shift

$$\Delta T_m \simeq 2l\frac{c_l - c_t}{c_l c_t} \tag{33}$$

in its period, with respect to the P wave. Moreover, the seismographs' recordings are local, i.e. the components of the displacement (velocity, acceleration) are recorded along local directions (for instance North-South, West-East and the vertical direction). In general, each of these components is a superposition of P and S waves, such that their spectrum exhibits, in general, two maxima. The length l_0 can be determined as an average value corresponding to these two maxima (for each direction, or as an average over directions).

Let us multiply the first row in Equation (31) by $\sin\omega t'$ and integrate over ω:

$$\int d\omega u_s(\omega) \sin\omega t' = u_0 l \int_{-T/2}^{T/2} dt\delta'(t) \int d\omega \sin\omega t \sin\omega t' \tag{34}$$

in this equation we use the well-known identity

$$\int d\omega \sin\omega t \sin\omega t' = \pi \left[\delta(t-t') - \delta(t+t')\right] \tag{35}$$

such that we get

$$\int d\omega u_s(\omega) \sin\omega t' = 2\pi u_0 l \delta'(t') \tag{36}$$

It follows that the seismic displacement (of the primary waves) has the Fourier components

$$u_s(\omega) \sin\omega t = -2cu_0 \sin\frac{\omega l}{2c} \sin\omega t \tag{37}$$

similarly, the acceleration $a_s(t)$ of the primary waves has the Fourier components

$$a_s(\omega) \sin\omega t = 2c\omega^2 u_0 \sin\frac{\omega l}{2c} \sin\omega t \tag{38}$$

These Fourier components can be used in studying the effect of monochromatic perturbations on the structures built on the Earth's surface.

6. Main shock

We pass now to the effects produced by the seismic main shock. On the Earth's surface the P and S seismic waves generate a main shock, which looks like two superposesd abrupt walls, with a long tail, propagating with the velocities of the elastic waves [16]. For a point placed on the Earth's surface at distance r from the epicentre we have for a primary seismic wave with extension l

$$R^2 = r^2 + z_0^2 \ , \ (R+l)^2 = (r+\Delta r)^2 + z_0^2 \tag{39}$$

where z_0 is the depth of the focus and

$$\Delta r = \frac{2Rl + l^2}{r + \sqrt{r^2 + 2Rl + l^2}} \tag{40}$$

resulting from these equations is the spread of the seismic spot left on the Earth's surface by the wave (**Figure 2**). Near the epicentre ($r \to 0$) the width of the seismic spot $\Delta r \simeq \sqrt{2z_0 l}$ is much larger than l ($l \ll z_0$). The distance $\sqrt{2z_0 l}$ defines an epicentral region. From Equation (39) we get the velocities $v_{l,t} = dr/dt = c_{l,t}\frac{R}{r}$ of the seismic spot on Earth's surface for distances $r \gg \Delta r$. We can see that these velocities are greater than the velocities of the elastic waves.

The displacement produced by the main shock on the Earth's surface is given by [16,17]

$$u_r = \theta(c_l\tau - r)\frac{\chi_0 r}{4c_l}\frac{\tau}{(c_l^2\tau^2 - r^2)^{3/2}} \ ,$$

$$u_\varphi = -\theta(c_t\tau - r)\frac{h_{0z} r}{4c_t}\frac{\tau}{(c_t^2\tau^2 - r^2)^{3/2}} \ , \tag{41}$$

$$u_z = \theta(c_t\tau - r)\frac{h_{0\varphi}}{4c_t r}\frac{c_t^2\tau^3}{(c_t^2\tau^2 - r^2)^{3/2}}$$

where r is the distance from the epicentre to the observation point on the Earth's surface, $\tau = t(1-\varepsilon)$, $\varepsilon = R/r-1$ and the potentials χ_0 and $h_{0\varphi,z}$ are of the order $\overline{M}/\rho R$, where $\overline{M}$ is the magnitude of the seismic moment. The coordinates r, φ, z are cylindrical coordinates. The time t in Equation (41) is measured from the moment each wave reaches the epicentre. We note that the main shock moves with velocities $c_{l,t}$, which are smaller than the velocities $v_{l,t} = c_{l,t}R/r$ of the intersections of the P and S waves with the Earth's surface. The main shock moves behind the P and S waves. Equation (41) are valid for a constant $\varepsilon < 1$ and within a limited range of the order z_0 for distances r, centered on a distance of the order z_0, where z_0 is the depth of the focus. We take the lower bound $r = z_0/\sqrt{3}$ corresponding to $\varepsilon = 1$. For smaller r the main shock is not yet well formed. For large epicentral distances the main shock is gradually diminishing. We may take $r = 2z_0$ as an upper bound. The boundaries of the region $z_0/\sqrt{3} < r < 2z_0$ where the main shock exists are approximate [18]. The singularity at $c_{l,t}\tau = r$ is smoothed out according to the replacement $c_{l,t}^2\tau^2 - r^2 \mid_{c_{l,t}\tau=r} \rightarrow r^2\varepsilon$, arising from the approximation $v_{l,t} = constant$.

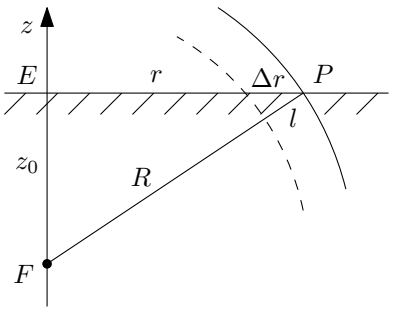

Figure 2. The spot of a primary seismic wave on the Earth's surface (focus F, epicentre E, observation point P).

For our practical purposes we may use the simplified formulae

$$u_r = -u_\varphi = \frac{\overline{M}r}{4\rho cR}g(\tau)\ ,\ u_z = \frac{\overline{M}}{4\rho rR}h(\tau) \tag{42}$$

where

$$g(\tau) = \frac{\theta(c\tau - r)\tau}{(c^2\tau^2 - r^2)^{3/2}}\ ,\ h(\tau) = \frac{\theta(c\tau - r)c\tau^3}{(c^2\tau^2 - r^2)^{3/2}} \tag{43}$$

In deriving the above formulae it is assumed that the sources of the secondary waves are sharply distributed over the surface; they are represented by spatial δ-functions [16]. Therefore, besides the cutoff length $r\sqrt{\varepsilon}$ given above, we have another cutoff length l, as arising from the spatial δ-function. The combined effect of the two cutoff lengths is given by $lr\sqrt{\varepsilon}/(l + r\sqrt{\varepsilon})$, which is approximately l, since $l \ll r\sqrt{\varepsilon}$. Therefore, we should use the cutoff length l in smoothing out the singularities occurring in the functions $g(\tau)$ and $h(\tau)$. By doing so, we get the peak values for the main shock displacement, velocity and acceleration

$$u_{max}^{ms} \simeq \frac{l^{3/2}r^{1/2}}{2R}\ ,\ v_{max}^{ms} \simeq \frac{3cl^{1/2}r^{1/2}}{4R}\ ,$$
$$a_{max}^{ms} \simeq \frac{15c^2r^{1/2}}{8l^{1/2}R} \tag{44}$$

(for all components), where the focal volume l^3 is used ($\overline{M} = 4\sqrt{2}\rho c^2 l^3$). These values are larger by a factor $(r/l)^{1/2}$ than the correspondig values of the primary waves (Equation (5)). If we take into account the energy loss, the factor $l^{3/2}$ in the displacement given above should be replaced by $l^3/l_0^{3/2}$, and the peak velocity and the peak acceleration are obtained from the peak displacement by using the factor c/l_0. We get

$$u_{max}^{ms} \simeq \frac{l^3 r^{1/2}}{2l_0^{3/2}R} \ , \ v_{max}^{ms} \simeq \frac{3cl^3 r^{1/2}}{4l_0^{5/2}R} \ , \qquad a_{max}^{ms} \simeq \frac{15c^2 l^3 r^{1/2}}{8l_0^{7/2}R} \tag{45}$$

These are the peak values produced by the main shock on the Earth's surface.

7. Response to the main shock

If we take the origin of the time at r/c and neglect the small scale factor $1-\varepsilon$, the displacement produced by the main shock has the general from

$$u_{ms} = \theta(t) f(t) \tag{46}$$

where the function $f(t)$ is given by Equations (42) and (43) (functions $g(t)$and $h(t)$). According to our discussion above, the ground motion, under the action of the seismic main shock, is given by the equation

$$\ddot{u}_g + \omega_g^2 u_g + 2\gamma_g \dot{u}_g = -\ddot{u}_{ms} = -\dot{f}(0)\delta(t) - f(0)\delta'(t) - \theta(t)\ddot{f}(t) \tag{47}$$

Therefore, the ground-motion displacement will include $-\dot{f}(0)G(t)$ and $-f(0)\dot{G}(t)$, where $G(t)$ is the Green function given by Equation (15); $f(0)$ and $\dot{f}(0)$ stand for the maximum displacement u_{max}^{ms} and the maximum velocity v_{max}^{ms} given by Equation (44). We can see that the factor $\theta(t)$ is present in the ground-motion displacement. The long tail of the main shock is now replaced by the effect of the damping coefficient. The solution u_g generates inertial forces for a seismograph, which will record the displacement step-function, specific to the main shock, with superposed oscillations.

Let us denote by $u_g^{(1)}$ the solution of Equation (47) corresponding to the first two (singular) terms ($\sim \delta(t), \delta'(t)$). It is easy to see that this solution leads to the peak values

$$u_{gmax}^{(1)} = u_{max}^{ms}\left(1 + 3c/2l_0\omega_g\right) \ , \qquad v_{gmax}^{(1)} = v_{max}^{ms}\left(1 + 2l_0\omega_g/3c\right) \ , \qquad a_{gmax}^{(1)} = a_{max}^{ms}\frac{2l_0\omega_g}{5c}\left(1 + 2l_0\omega_g/3c\right) \tag{48}$$

For the last term in Equation (47) a particular solution is $-\ddot{w}$, where w satisfies the equation

$$\ddot{w} + \omega_g^2 w + 2\gamma_g w = f(t) \tag{49}$$

for $t > 0$. For the general solution $u_g^{(2)}$ we add a solution of the free equation

and impose vanishing initial conditions. This procedure is equivalent with the Green function procedure described previously. A particular solution of Equation (49) is obtained by Fourier transformation. We find easily that it is given by

$$w = -\frac{1}{\omega_g} Im\left[f(\omega_g)e^{-i\omega_g t}\right] e^{-\gamma_g t} \tag{50}$$

such that

$$u^{(2)} = -\omega_g Im\left[f(\omega_g)e^{-i\omega_g t}\right] e^{-\gamma_g t} \tag{51}$$

Therefore, in order to find out the response to the seismic main shock, we need the Fourier transform of the displacement of the main shock. This amounts to the Fourier transforms of the functions $g(t)$ and $h(t)$ given by Equation (43).

For the Fourier transform of the function $g(t)$ we have

$$\begin{gathered} g(\omega) = \int_{r/c}^{\infty} dt \frac{t}{(c^2t^2-r^2)^{3/2}} e^{i\omega t} = \\ = \frac{1}{\sqrt{2}c^2 l^{1/2} r^{1/2}} e^{i\omega r/c} - \frac{\pi\omega}{2c^3} H_0^{(1)}(\omega r/c) \end{gathered} \tag{52}$$

where $H_0^{(1)}$ is the Hankel function of the first kind and zeroth order [21]. For all epicentral distances of interest we may use the asymptotic form of the Hankel function $H_0^{(1)}(\omega r/c) \simeq \sqrt{\frac{2c}{\pi\omega r}} e^{i(\omega r/c - \pi/4)}$. It follows that the response $u^{(2)}$ (Equation (51)) is a superposition of (damped) waves $\sin\omega_g(t - r/c)$ and $\cos\omega_g(t - r/c)$. A similar estimation is valid for $h(\omega)$. Also, from Equation (52) we can see that the amplitude of a component wave in the ground motion has a maximum for a frequency of the order $\omega_g \lesssim c/l$, which would indicate a (pseudo-) resonance for the characteristic frequency of the seismic motion, a rather improbable situation.

By making use of Equations (42), (51) and (52) it is easy to find the peak values corresponding to this contribution:

$$\begin{gathered} u_{gmax}^{(2)} = 2u_{max}^{ms} \frac{l_0\omega_g}{c} \left(1 + \sqrt{\pi l_0\omega_g/2c}\right) \ , \\ v_{gmax}^{(2)} = \frac{4}{3} v_{max}^{ms} \left(\frac{l_0\omega_g}{c}\right)^2 \left(1 + \sqrt{\pi l_0\omega_g/2c}\right) \ , \\ a_{gmax}^{(2)} = \frac{8}{15} a_{max}^{ms} \left(\frac{l_0\omega_g}{c}\right)^3 \left(1 + \sqrt{\pi l_0\omega_g/2c}\right) \end{gathered} \tag{53}$$

These quantities are approximately the corresponding quantities given by Equation (48) multiplied by a factor $(l_0\omega_g/c)^2$. As discussed above (after Equation (22)), we consider the parameter $l_0\omega_g/c$ of the order of unity at most. Therefore, these contributions are at most of the same order as the corresponding contributions given by Equation (48). It follows that for seismic hazard studies we may use Equation (48). From Equations (45) and (48) we get the peak values of the ground motion caused by

the mainshock

$$u_{gmax}^{ms} = \frac{3cl^3r^{1/2}}{4\omega_g l_0^{5/2}R}\left(1 + 2l_0\omega_g/3c\right) \ ,$$

$$v_{gmax}^{ms} = \frac{3cl^3r^{1/2}}{4l_0^{5/2}R}\left(1 + 2l_0\omega_g/3c\right) \ , \tag{54}$$

$$a_{gmax}^{ms} = \frac{3c\omega_g l^3r^{1/2}}{4l_0^{5/2}R}\left(1 + 2l_0\omega_g/3c\right)$$

This is the last set of basic equations we need. It is worth noting that the ground-motion peak acceleration is smaller than the peak acceleration of the main shock which caused that ground motion. These equations should be applied over the validity region of the main shock, *i.e.* from approximately $r = z_0/\sqrt{3}$ to $r = 2z_0$, according to the above discussion, where z_0 is the depth of the earthquake focus. The results given by Equation (54) should be compared to the peak values of the ground motion caused by the primary waves (Equation (23)). It is easy to see that u_{gmax}^{ms} and v_{max}^{ms} are dominant values, while for acceleration we need to take the maximum between a_{gmax}^{ms} and a_{max}^{p} given by Equation (23). This maximum value depends on the ratio of the quantities $l_0\omega_g/c$ and $(l_0/r)^{1/2}$ (both smaller than unity). Outside the region where the main shock is present the ground-motion peak values are those corresponding to the primary waves, as given by Equation (23). All these results can be written as follows:

For $z_0/\sqrt{3} < r < 2z_0$

$$u_{gmax} = \frac{3cl^3r^{1/2}}{4\omega_g l_0^{5/2}R}\left(1 + 2l_0\omega_g/3c\right) \ ,$$

$$v_{gmax} = \frac{3cl^3r^{1/2}}{4l_0^{5/2}R}\left(1 + 2l_0\omega_g/3c\right) \ , \tag{55}$$

$$a_{gmax} = max\left\{a_{gmax}^{ms} \ , \ a_{gmax}^{p}\right\}$$

where

$$a_{gmax}^{ms} = \frac{3c\omega_g l^3r^{1/2}}{4l_0^{5/2}R}\left(1 + 2l_0\omega_g/3c\right) \ ,$$

$$a_{gmax}^{p} = \frac{\sqrt{2}c^2l^3}{\pi l_0^3R}\left(1 + l_0^4\omega_g^4/c^4\right) \tag{56}$$

outside this region (except for the epicentral region of radius $\sqrt{2z_0l_0}$)

$$u_{gmax} = \frac{\sqrt{2}l^3}{\pi l_0R}\left(1 + l_0^2\omega_g^2/c^2\right) \ ,$$

$$v_{gmax} = \frac{\sqrt{2}cl^3}{\pi l_0^2R}\left(1 + l_0^3\omega_g^3/c^3\right) \ , \tag{57}$$

$$a_{gmax} = \frac{\sqrt{2}c^2l^3}{\pi l_0^3R}\left(1 + l_0^4\omega_g^4/c^4\right)$$

Such equations can be used for estimating the peak values of the ground motion.

8. Response to a monochromatic oscillation

Besides the discontinuous, or singular components of the seismic ground-motion, seismographs or structures built on the Earth's surface, viewed as linear harmonic oscillators with frequency ω_s and damping coefficient γ_s, are subjected to monochromatic oscillations with frequency ω_g (and damping coefficient γ_g). For reference, we include here the well-known response of the oscillator to a monochromatic external force. The equation which governs the oscillator's displacement can be written as

$$\ddot{u} + \omega_s^2 u + 2\gamma_s \dot{u} = a_g(t) \tag{58}$$

where u is the displacement and $a_g(t)$ is the (minus) acceleration generated by the ground motion (a coupling impedance can also be introduced). We adopt an external acceleration corresponding to the function $a_g(t) = a_0(\omega_g)\sin\omega_g t$, given by the site response calculated above (leaving aside the damping coefficient γ_g). The above equation is viewed as being defined for $t > 0$, with vanishing initial conditions. The solution is obtained by adding the free solution to a particular solution. By doing so, we get

$$\begin{aligned} u(t) = a_0(\omega_g)\tfrac{\omega_g^2-\omega_s^2}{(\omega_g^2-\omega_s^2)^2+4\omega_g^2\gamma_s^2}\left(\tfrac{\omega_g}{\omega_s}e^{-\gamma_s t}\sin\omega_s t - \sin\omega_g t\right) + \\ +a_0(\omega_g)\tfrac{2\omega_g\gamma_s}{(\omega_g^2-\omega_s^2)^2+4\omega_g^2\gamma_s^2}\left(e^{-\gamma_s t}\cos\omega_s t - \cos\omega_g t\right) \end{aligned} \tag{59}$$

We can see that the solution given by Equation (59) exhibits a resonance for $\omega_g = \omega_s$, attenuated by the damping. At resonance, $u(t) = -\frac{a_0(\omega_s)}{2\omega_g\gamma_s}\left(1 - e^{-\gamma_s t}\right)\cos\omega_s t$. The ratio $\mid u(\omega_s)/a_0(\omega_s) \mid$, where $u(\omega_s)$ is the Fourier transform of $u(t)$ for large values of t, leads to an amplification factor of the order $1/\omega_g\gamma_s$ for displacement and ω_g/γ_s for acceleration.

The energy conservation resulted from Equation (58) is

$$\frac{d}{dt}\left(\frac{1}{2}\dot{u}^2 + \frac{1}{2}\omega_s^2 u^2\right) + 2\gamma_s\dot{u}^2 = F\dot{u} \tag{60}$$

where $\mathcal{E} = \frac{1}{2}\dot{u}^2 + \frac{1}{2}\omega_s^2 u^2$ is the energy of the oscillator, $W = 2\gamma_s\dot{u}^2$ is the energy dissipated per unit time and $F\dot{u}$ is the work done by the force $F(t) = a_g(t)$ per unit time (all quantities per unit mass). The oscillator receives energy from the external source and dissipates it. For large values of t the displacement of the oscillator is

$$\begin{aligned} u(t) = -a_0(\omega_g)\{\tfrac{\omega_g^2-\omega_s^2}{(\omega_g^2-\omega_s^2)^2+4\omega_g^2\gamma_s^2}\sin\omega_g t + \\ +\tfrac{2\omega_g\gamma_s}{(\omega_g^2-\omega_s^2)^2+4\omega_g^2\gamma_s^2}\cos\omega_g t\} \end{aligned} \tag{61}$$

The average energy of the oscillator is

$$\overline{\mathcal{E}} = \frac{1}{4}a_0^2\frac{\omega_g^2+\omega_s^2}{(\omega_g^2-\omega_s^2)^2+4\omega_g^2\gamma_s^2} \tag{62}$$

the average energy dissipated per unit time is

$$\overline{W} = \overline{2\gamma_s \dot{u}^2} = a_0^2 \frac{\gamma_s \omega_g^2}{(\omega_g^2 - \omega_s^2)^2 + 4\omega_g^2 \gamma_s^2} \tag{63}$$

and the average work done by the external force per unit time is equal to the dissipated energy per unit time ($\overline{F\dot{u}} = \overline{W}$); indeed, the rate of the average energy of the oscillator is zero. At resonance $\overline{\mathcal{E}} = a_0^2/8\gamma_s^2$, $\overline{W} = \overline{F\dot{u}} = a_0^2/4\gamma_s$. We can see that for low damping at resonance the amplification and the energy is high, while the dissipation is lower than the energy.

Finally, we note that the acceleration of the primary waves has monochromatic components of the form $a_0(\omega) \sin \omega t$, where

$$a_0(\omega) = 2cu_0\omega^2 \sin \omega l/2c \tag{64}$$

according to Equation (38). Therefore, under the action of this acceleration, the displacement of the oscillator is given by the above formulae. Far from resonance the response of the oscillator does not differ appreciably from the seismic spectrum (Equation (59)); the frequency of the maximum amplitude remains at $\omega_m \simeq \pi c/l$ (for displacement). On the contrary, close to resonance the response is given approximately by

$$u(t) \simeq -cu_0 \frac{\omega_s^2 \gamma_s}{(\omega - \omega_s)^2 + \gamma_s^2} \sin \omega_s l/2c \cos \omega_s t \tag{65}$$

where we can see that the response is maximal for the resonance frequency ω_s.

For an elastic, vertical bar, with length L, the lower end embedded in the ground and the upper end free, we may take as eigenfrequencies $\omega_n = \frac{(2n+1)\pi}{2} \frac{c}{L}$, where c is the velocity of the elastic waves in the bar and $n = 0,\ 1,\ 2....$ The seismic acceleration of the primary waves has a narrow peak for, approximately, $\omega_m \simeq \frac{3\pi}{2} \frac{c_{l,t}}{l}$. It follows that the resonance is avoided for $L \neq (2n+1)\frac{c}{3c_{l,t}} l$. A similar conclusion is valid for a site in resonance with the main shock, where ω_g is of the order of the characteristic frequency c/l of the seismic motion, a rather improbable case.

9. Concluding remarks

The seismic motion produced by an earthquake (in a homogeneous and isotropic medium) consists of the primary P and S seismic waves, followed by two abrupt walls with a long tail, which form the seismic main shock. The primary waves are spherical-shell waves with a scissor-like shape. The local effects of this motion on the Earth's surface depend on the elastic particularities of the site. The resulting motion of the site is the ground motion. The estimation of the peak values of the displacement, velocity and acceleration of the ground motion is the central target of seismic hazard studies. We use a model of linear harmonic oscillator for the site, with an eigenfrequency and a damping coefficient, subject to the seismic motion. The resulting ground motion consists of damped oscillations with the site frequency (the response of the site), superposed over the original seismic motion. The peak values of the displacement, the velocity and the acceleration of the ground motion are estimated

in this paper. These values depend on the focal distance R, the epicentral distance r, the eigenfrequency ω_g of the site and two parameters l and l_0. The parameter l is of the order of the dimension of the focus, while the parameter l_0, larger than l, is the average width of the spot the primary waves leave on the Earth's surface.

The ground motion acts like an external force upon seismographs and structures built on the Earth's surface, viewed as linear harmonic oscillators. The motion of these oscillators consists of damped oscillations with their own eigenfrequencies, damped oscillations with the ground-motion frequency (the response), superposed over the original seismic motion (contained in the ground motion). The seismograms preserve the scissor-like shape of the primary waves, possibly deformed by the interplay of the intervening frequencies, as well as the abrupt wall-like shape of the main shock, with damped oscillations. From the Fourier transforms of the seismograms we can read the parameters ω_g and l_0. We note that ω_g characterizes the site, while l_0 characterizes the elastic medium. Also, we expect a small dependence on site and magnitudes of the ratio l/l_0. For strong seismic motion the non-linearities may cause an appreciable dependence on magnitudes both of l_0 and ω_g. The parameter l is determined from the magnitude of the expected earthquake (Equation (6)).

The peak values of the ground motion are given by Equations (55) and (57). As discussed above we assume $l_0\omega_g/c < 1$, where c is the average velocity of the elastic seismic waves (for instance, $c = 5$ km/s). The parameter l (the dimension of the focus in cm) is provided by Equation (6),

$$\lg l = \frac{1}{2}M_w + 1 \tag{66}$$

where M_w is the moment magnitude of the earthquake (for $\rho = 5$ g/cm^3 and $c = 5$ km/s). The eigenfrequency ω_g, which characterizes the site, can be determined from the spectral analysis of the ground-motion response (seismograms, *e.g.* Equation (27) for the primary waves, or Equations (47) and (51) for the main shock). The parameter l_0 is given by the frequency $\omega_m = \pi c/l_0$ of the maximum of the Fourier transform of the primary wave displacement recorded by seismograms, according to Equation (31) (or the maximum of the velocity, the acceleration). For consistency, the inequality $l_0 > l$ should be satisfied, i.e.

$$T_m > \frac{20}{c}10^{M_w/2} \tag{67}$$

where T_m is the period corresponding to the frequency ω_m.

A survey of a few tens of moderate Vrancea earthquakes (magnitude $M_w = 3.5-5$, average focal depth $\simeq 100$ km) shows $l/l_0 \simeq 1/10$. Let us supose that we are interested in an earthquake with magnitude $M_w = 7$. According to Equation (66) the focus dimension is $l = 316$ m and, consequently, $l_0 = 3.16$ km. For $\omega_g = 1$ s^{-1} we get $l_0\omega_g/c \simeq 0.63$ ($c = 5$ km/s). Let us assume that the focal depth is $z_0 = 100$ km and we are interested in the ground motion produced by this earthquake at the epicentral distance $r = 100$ km ($R = 100\sqrt{2}$ km). Therefore, we use Equation (55), which give $a^{ms}_{gmax} = 67$ cm/s^2 and $a^{p}_{gmax} = 9$ cm/s^2. It follows the peak values of the ground motion $u_{gmax} = 67$ cm, $v_{gmax} = 67$ cm/s and $a_{gmax} = 67$ cm/s$^2 \simeq 0.07$ g (where $g = 980$ cm/s^2 is the gravitational acceleration).

Funding: This work was carried out within the Program Nucleu SOL4RISC, funded by the Romanian Ministry of Research, Innovation and Digitization, contract no. 24N/03.01.2023, project no. PN23360202.

Acknowledgments: The author is indebted to the colleagues in the Institute of Earth's Physics, Magurele-Bucharest, and to L. C. Cune for many enlightening discussions.

Conflict of interest: The author declares no conflict of interest.

References

1. McGuire RK. Seismic Hazard and Risk Anaylsis. Earthquake Engineering Research Institute. 2004.
2. Hanks TC, McGuire RK. The character of high-frequency strong ground motion. Bull. Seism. Soc. Am. 1981; 71: 2071–2095.
3. Boore DM. Stochastic simulation of high-frequency ground motion based on seismological models of the radiated spectrum. Bull. Seism. Soc. Am. 1983; 73: 1865–1894.
4. Boore DM. Simulation of ground motion using the stochastic method. Pure and Appl. Geophys. 2003; 160: 635–676.
5. Bora SS, Scherbaum F, Kuehn N, Stafford P. On the relationship between Fourier and response spectra: Implications for the adjustment of empirical ground-motion prediction equations (GMPEs). Bull. Seism. Soc. Am. 2016; 1235–1253.
6. Chavez-Garcia FJ. Site effects: From observation and modelling to accounting for them in building codes. In: Pitilakis KD (editors). Earthquake Geotechnical Engineering. Geotechnical, Geological and Earthqauke Engineering. Springer; 2007. volume 6.
7. Kumar S, Kumar D, Rastogl B. Source parameters and scaling relations for small earthquakes in the Kachchh region of Gujarat, India. Nat. Hazards. 2014; 73: 1269–1289.
8. Pagliaroli A, Aprile V, Chamlagain D, et al. Assessment of site effects in the Kathmandu valey, Nepal, during the 2015 M_w 7.8 Gorkha earthquake sequence using 1D and 2D numerical modelling. Eng. Geol. 2018; 239: 50–62.
9. Bashir K, Debnath R, Saha R. Estimation of local site effects and seismic vulnerability using geotechnical dataset at flyover site Agartala India. Acta Geophys. 2022; 70: 1003–1036.
10. El-Nabulsi RA, Anukool W. Fractal dimension modelling of seismology and earthquake dynamics. Acta Mech. 2022; 233: 2107–2122.
11. Atkinson G, Boore D. Ground-motion relations for Eastern North America. Bul. Seism. Soc. Am. 1995; 85: 17–30.
12. Atkinson G, Boore D. Earthquake ground-motion prediction equations for Eastern North America. Bul. Seism. Soc. Am. 2006; 96: 2181–2205.
13. Atkinson G. Ground-motion prediction equations for Eastern North America from a referenced empirical approach: Implications for epistemic uncertainty. Bul. Seism. Soc. Am. 2008; 98: 1304–1318.
14. Baker JW, Bradley BA, Stafford PJ. Seismic Hazard and Risk Analysis. Cambridge University Press; 2021.
15. Apostol BF. Elastic displacement in a half-space under the action of a tensor force. General solution for the half-space with point forces. J. Elas. 2017; 126: 231–244.
16. Apostol BF. Elastic waves inside and on the surface of a half-space. Quart. J. Mech. Appl. Math. 2017; 70: 289–308.
17. Apostol BF. An inverse problem in seismology: Derivation of the seismic source parameters from P and S seismic waves. J. Seism. 2019; 23: 1017–1030.
18. Apostol BF, Cune LC. A Guide to Practical Seismology. Cambridge Scholars Publishing; 2023.
19. Apostol M. Singular Equations of Waves and Vibrations. Cambridge Scholars Publishing; 2023.
20. Brune JN. Tectonic stress and the spectra of seismic shear waves for earthquakes. J. Geophys. Res. 1970; 75: 4997–5009.
21. Gradshteyn IS, Ryzhik IM, Jeffrey A, Zwillinger D. Tables of Integrals, Series and Products, 6th ed. Academic Press; 2000. p. 904.